Comparative numerical study to simulate masonry with bed joint reinforced repointing

Ho Lee, Ka; Mehrotra, Anjali; Esposito, Rita

DOI
10.1016/j.engstruct.2023.117135

Publication date
2023

Document Version
Final published version

Published in
Engineering Structures

Engineering Structures 300 (2024) 117135

Contents lists available at ScienceDirect

Engineering Structures

journal homepage: www.elsevier.com/locate/engstruct

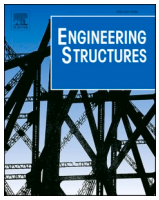

Comparative numerical study to simulate masonry with bed joint reinforced repointing

Ka Ho Lee, Anjali Mehrotra, Rita Esposito *

Faculty of Civil Engineering and Geosciences, Delft University of Technology, the Netherlands

ARTICLE INFO

Keywords:
Unreinforced masonry
Bed joint reinforced repointing
Continuum damage model
Brick-to-brick models
Comparative numerical study

ABSTRACT

Bed joint reinforced repointing is a retrofitting technique for unreinforced masonry structures that is commonly applied in the Netherlands to repair settlement-induced damage. Using this technique, the bed joints of masonry walls are reinforced with steel rebars that are embedded in a high strength repair mortar. Due to the increase of induced seismic events in the northern part of the Netherlands, an experimental study was carried out at Delft University of Technology to investigate the performance of this retrofitting technique for combined settlement and seismic loading. This paper aims to simulate the experimental results, with a focus on the comparison of different finite element modelling approaches for studying both un-strengthened and strengthened full-scale tested walls. To that end, three different models are investigated – comprising both macro (continuum) and simplified and detailed micro (brick-to-brick) modelling approaches. The bricks and mortar joints are modelled as one homogenous continuum in the macro model, whereas in the two brick-to-brick models these structural components are modelled separately, with the detailed model including interface elements to simulate the brick–mortar bonds. Nonlinear pushover analyses are subsequently carried out using all three modelling approaches, for both monotonic and cyclic loading cases. Based on these analyses, the detailed brick-to-brick model was found unsuitable to simulate the strengthened wall because cracks in the model mainly occur in the form of opening of the brick–mortar bond interfaces, while smeared cracking in the plane stress elements of the mortar joints is very limited. Similarly, the continuum damage model was found to be inaccurate when pre-existing damage in the experiment needed to be taken into account. The continuum damage model also showed lower axial stresses in the rebars, compared with the simplified brick-to-brick model, as the former does not allow for the direct assignment of material properties for the high strength repair mortar in the strengthened joints.

1. Introduction

The extraction of natural gas in the region of Groningen in the northern part of the Netherlands has been causing human-induced seismic activities for the past several decades [8]. This is problematic as the existing building stock in this region, which consists of mainly unreinforced masonry buildings and historical structures, is not designed to withstand seismic events as evidenced by a lack of empirical earthquake-resistant design features. Specifically, the presence of large openings and relatively slender walls makes these structures vulnerable to damage under the influence of seismic action. Further, a number of these buildings often sit on soft topsoil, which when combined with the gas extraction, is responsible for ground settlements which may further compromise their seismic capacity.

A large number of experimental and numerical campaigns have been carried out at Delft University of Technology to understand the response of these unreinforced masonry (URM) structures to induced earthquakes [20], including several full-scale in-plane seismic tests on masonry walls [21] & [19,12]. One field of the experiments focused on the application and assessment of a retrofitting technique, namely *bed joint reinforced repointing*. This retrofitting technique consists of cutting a slot in the bed joints and installing steel bars, embedded in a high-strength repair mortar. Although this method is commonly applied in the Netherlands to counteract settlement damage, limited investigations have been conducted on its performance against seismic loading. To that end, an experimental campaign was conducted in which a quasi-static cyclic in-plane test on a full-scale masonry wall was performed to characterize the performance of the bed joint reinforcement technique [3,4,14,28]. Compared to the un-strengthened walls, tested in a previous experimental campaign under similar conditions [10], it was observed that the

* Corresponding author.
E-mail address: r.esposito@tudelft.nl (R. Esposito).

https://doi.org/10.1016/j.engstruct.2023.117135
Received 25 July 2023; Received in revised form 18 October 2023; Accepted 5 November 2023
Available online 20 November 2023

bed joint reinforced repointing can provide a significant improvement in terms of the displacement capacity and ductility of the wall, but not the force capacity.

Previously, Drougkas and co-authors ([3] & [4]) performed numerical investigations using both the *continuum damage model* (bricks and mortar joints modelled as one homogeneous continuum) and the *simplified brick-to-brick model* (bricks and mortar joints modelled separately) for the simulation of the full-scale walls from the experiments. For both modelling approaches, an orthotropic smeared continuum model [26,27], was used for the simulation of the strengthened wall up to the Near Collapse state (that is, the state where the structure sustained heavy damage, close to structural collapse). It was observed that the bed joint bars below the window opening developed the highest axial stresses, without reaching yielding. Furthermore, Korswagen and co-authors ([10] & [11]) also used the two aforementioned modelling approaches and performed several numerical simulations of the un-strengthened wall in the Damage Limitation state (that is, the state where the structure sustained visible, "light" but repairable damage as is typical of low-magnitude, shallow earthquakes). It was reported that the strength and stiffness degradation observed in the experiments was not reproduced by the models using the orthotropic model. Moreover, when applying a monotonic loading protocol, the *simplified brick-to-brick model* was found to be more stable than the *continuum damage model*, meaning that more fluctuations were observed in the force–displacement curve for the latter. On the other hand, the *detailed brick-to-brick model,* in which the bricks and mortar joints are modelled separately with line interface elements included at the brick–mortar bonds (e.g. [17,2]), has not yet been adopted to simulate the wall retrofitted with the bed joint reinforced repointing.

This paper focusses on the comparison of different modelling techniques to simulate the response of masonry walls retrofitted with bed joint reinforced repointing and also provides such a comparison for un-strengthened walls. To that end, nonlinear pushover analyses (monotonic and cyclic) are performed using the following three finite element modelling strategies: the *continuum damage model*, the *simplified brick-to-brick model* and *the detailed brick-to-brick model*. These approaches are chosen with respect to the ones available in literature, because they are the only one allowing for the integration of the reinforcement bars in the masonry or mortar elements. In this respect, for example the use of a model where the bricks are expanded up to half the thickness of the mortar joints, and connected to each other with zero-thickness interface elements (e.g., [15,23] & [24]) is not suitable since reinforcement bars cannot be connected to the zero-thickness interface elements. The objective of this study is to provide a comparison of the three aforementioned modelling approaches and to find the most suited one for the simulation of the un-strengthened and strengthened walls.

The comparative numerical study presented in this paper provides a better understanding of the challenges related to the modelling of strengthened masonry. In fact, often the modelling of strengthen masonry is address by using a single modelling technique with the purpose of replicating a set of experimental data. This is done either to understand the local response of the reinforcement (e.g., [7], [1]) or to support the development of new modelling strategies (e.g.,[22,9]).

The outline of this paper is as follows. First, a short summary of the experiment and test results is given in Section 2 as benchmark for the numerical simulations. Second, all aspects of the numerical modelling are discussed in Section 3. Third, the numerical results are presented and discussed in Section 4. Finally, the concluding remarks and limitations of this study are presented and discussed in Section 5.

2. Experimental benchmarks

In this paper two quasi-static cyclic in-plane tests on full-scale masonry walls performed at Delft University of Technology, are selected as benchmarks: an un-strengthened wall *TUD_COMP-41* [10] and a wall strengthened with bed joint reinforced repointing *TUD_COMP-45*

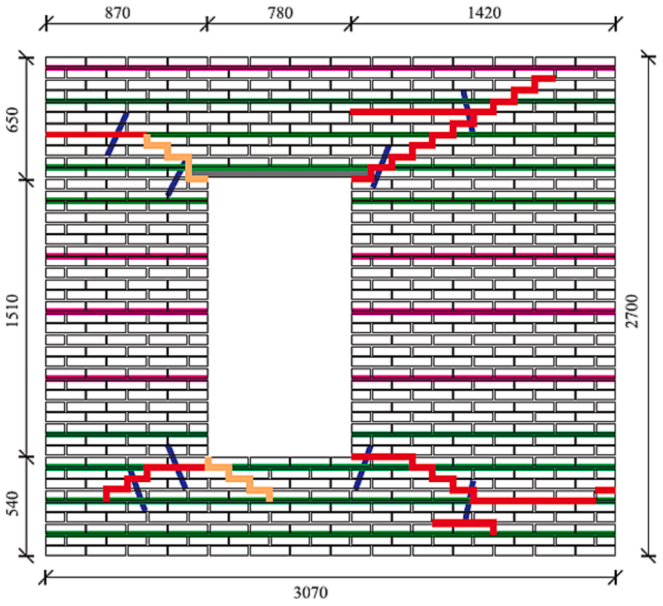

Fig. 1. Geometry of strengthened wall (TUD_COMP-45) with pre-damage (orange), post-damage (red), bed joint reinforcements (double bars in green and single bar in pink), diagonal ties (blue) [4]. (For interpretation of the references to colour in this figure legend, the reader is referred to the web version of this article.)

[14,28]. Both walls have the same geometry, material properties, loading and boundary conditions. The walls were built in single-leaf running bond using clay bricks and featured a single eccentrically located window opening. These walls represent slender walls with openings which are typically found in Dutch houses.

Both walls were tested in a cantilever configuration which allowed for free displacement and rotation of the top while the bottom was fully fixed. Moreover, both walls were tested in the Damage Limitation (DL) state as well as in the Near Collapse (NC) state. The DL state consisted of a repetitive (one-way cyclic) quasi-static loading phase, comprising five incremental cycles of 20 runs each in the positive loading direction, followed by a cyclic (two-way) quasi-static loading phase, comprising seven incremental cycles of 30 runs each in both loading directions. A run is defined as the loading sequence after which the target displacement is applied in one or both loading directions up to returning to the original position of the wall. The NC state was a cyclic (two-way) quasi-static loading phase, comprising eight cycles. The first two cycles consist of two runs each, while the remaining six cycles consist of one run each.

The bed joint reinforcements were embedded (single or double bar configuration) in a layer of high strength repair mortar, while the diagonal ties were placed in pilot holes which were drilled across the diaognal stair-case cracks (Fig. 1). To simulate the presence of existing damage due to settement, the strengthened wall featured artificially introduced cracks (referred to as pre-damage, orange lines in Fig. 1), achieved by the inclusion of plastic sheets between the bricks and mortar joints, to account for the absence of bonding between them. To simulate the presence of damage due to low-intensity earthquakes, the wall was then tested in its un-strengthened state up to the light damage (DL) state; with the obtained damage here referred to as post-damage (red lines in Fig. 1). Afterwards, the wall was strengthened with the bed joint reinforced repointing and tested up to near collapse (NC). Differently than the strengthened wall, pre-damage was not present in the un-strengthened wall. Consequently, the comparison for light damage state is made considering the wall *TUD_COMP-45* before and after the application of the retrofitting technique, while the comparison for the near collapse is made between the two different walls.

According to [14,28], a reduction of crack width and length was obtained at the end of the DL state for the strengthened wall and an

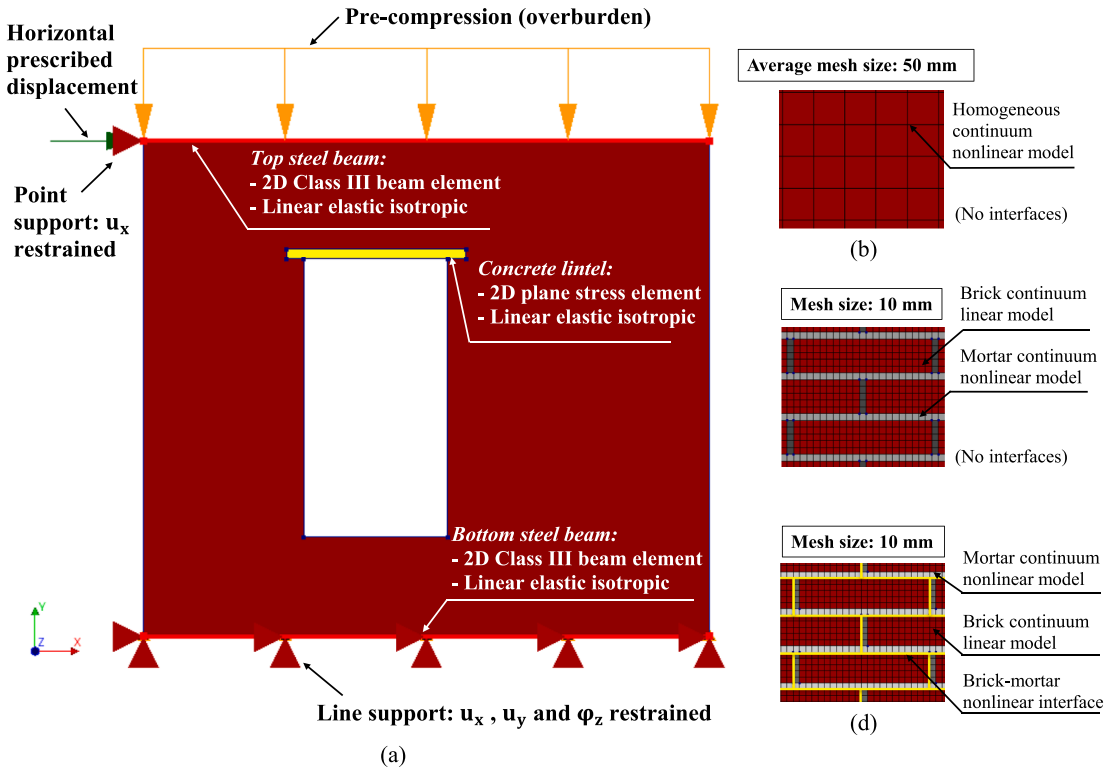

Fig. 2. (a) Finite element model of full-scale un-strengthened wall; (b) continuum damage model; (c) simplified brick-to-brick model; (d) detailed brick-to-brick model with line interface elements marked in yellow. (For interpretation of the references to colour in this figure legend, the reader is referred to the web version of this article.)

increase in displacement capacity was recorded for the NC state. Both the un-strengthened and strengthened walls showed similar crack patterns at the end of the DL state, namely cracks mainly developed stepwise in the mortar joints from the window corners. No significant increment in force capacity was observed. The effect of the bed joint reinforcements was more evident at the end of the NC state in terms of a significant increment in displacement capacity and ductility of the wall. Approaching the end of the test, the presence of the steel bars in the bed joints triggered an arch failure mechanism at the area underneath the window opening, and toe crushing at the bottom right corner of the wall. The experimental results are presented together with the numerical results in the next sections. For a more detailed description of these experiments the reader is referred to Licciardello et al. [28] and Drougkas et al., [4].

3. Numerical modelling methods

To simulate the experiments as described above, three different finite element modelling approaches are adopted in this paper, namely: the *continuum damage model;* the *simplified brick-to-brick model* and the *detailed brick-to-brick model* (Fig. 2). These models are adopted to simulate both the un-strengthened and strengthened full-scale masonry walls from the experiments. The numerical analyses have been performed using the finite element software DIANA version 10.4 [6]. Material properties used are listed in Table A1 and A2

The bricks and the mortar joints are modelled as one homogeneous continuum in the *continuum damage model,* where the material non-linearity is modelled using an orthotropic smeared cracking model to account for the orthotropic behavior of masonry [26,27]. This model assumes a linear softening in tension with secant unloading, a parabolic curve to describe the compressive behavior with non-secant unloading, and a linear softening in shear with elastic unloading and limitation of the maximum stress accordingly to Coulomb friction criterion. Plane stress elements with a mesh size of 50 mm are adopted for the masonry.

In the *simplified brick-to-brick model*, the bricks and mortar joints are modelled separately but fully bonded, since failure at brick–mortar interface is not modelled. The bricks are kept linear elastic since cracking was not observed in the bricks until the last cycle of the experiment. The material non-linearity in the mortar joints is modelled using the orthotropic material model as applied above (but now applied only in the mortar joints), while a second model is also created using an isotropic material model in the mortar joints. Differently from the orthotropic model, the isotropic model only allows for secant unloading in shear [25,26]. Moreover, as for the orthotropic model, a linear softening function in tension and a parabolic softening function in compression has been applied for the isotropic model. Plane stress elements are used for the bricks and mortar; the mesh size is set to 10 mm to match the thickness of the mortar joints.

Compared to the simplified brick-to-brick models, the only addition for the *detailed brick-to-brick model* is the inclusion of line interface elements at the brick–mortar bonds to account for the behavior over the discontinuous surfaces. These line interface elements are only placed at one side of the mortar joints which reduces the modelling effort and computational costs, without compromising the model accuracy [2]. As in the simplified brick-to-brick model, the bricks are kept linear elastic and the mortar is modelled adopting the orthotropic joint model; the same mesh size of 10 mm is used. The material non-linearity in the line interfaces at the brick–mortar bonds is modelled using a discrete cracking model including only tensile softening with secant unloading.

To account for pre- and post-damage, modified material properties are assigned. Specifically, the Young's modulus is reduced by 50 % compared to the un-damaged properties, while the tensile strength as well as the tensile and shear fracture energy are reduced to zero. This is done in order to account for the absence of bond in the pre-damage and the loss of interface cohesion in the post-damage due to crack opening [3]. For the continuum damage model, areas are identified for the

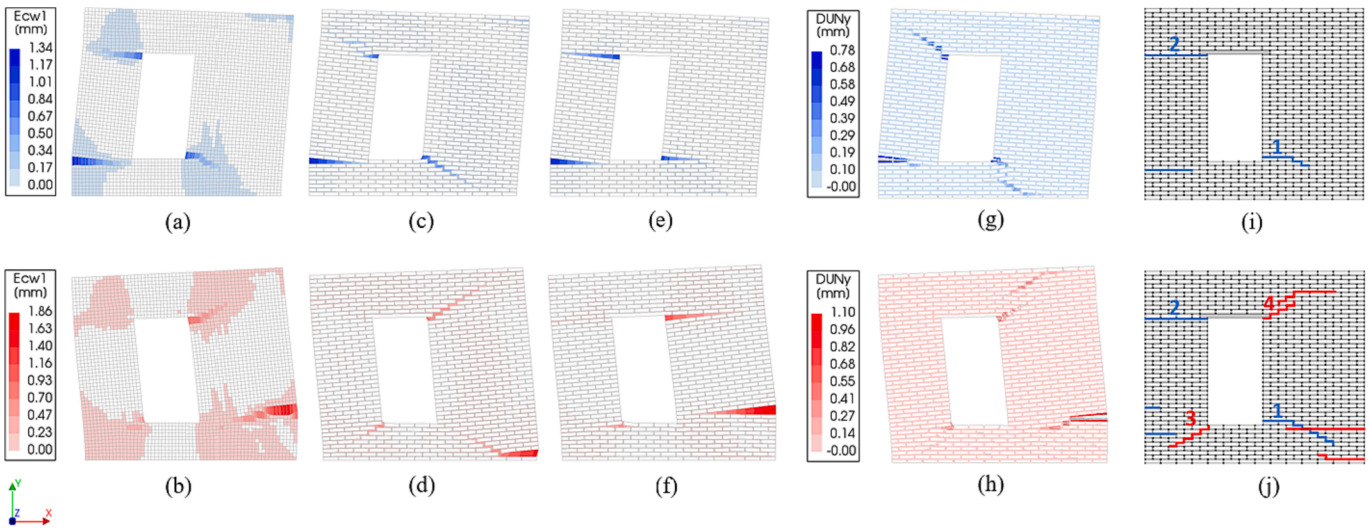

Fig. 3. Crack pattern in positive (blue) and negative (red) loading direction for un-strengthened wall in damage limitation phase: (a)-(b) continuum damage model; (c)-(d) simplified brick-to-brick model with isotropic joint model; (e)-(f) simplified brick-to-brick model with orthotropic joint model; (g)-(h) detailed brick-to-brick model; (i)-(j) experimental results (TUD_COMP-41). Ecw1 is the crack width in the maximum principal direction in plane stress elements and DUNy is the vertical crack opening in interface elements. (For interpretation of the references to colour in this figure legend, the reader is referred to the web version of this article.)

assignment of the reduced properties accordingly to the location of pre- and post-damage [3]. On the other hand, pre- and post-damage can be more accurately included in both the simplified and detailed brick-to-brick models since the bed and head joints are modelled individually, which allows for the direct assignment of the modified material properties to each structural component.

The steel reinforcing bars are simulated with truss elements (i.e. bar elements, allowing for only axial forces/deformations) where interface elements are incorporated between the trusses and the plane stress elements to simulate the bond-slip behavior. The Von Mises plasticity model is used to simulate potential yielding of the reinforcements in tension, while the bond-slip behavior is simulated by adopting the curve proposed by Model Code 2010 [5] and considering the related experimental results. The material properties and numerical parameters are based on the previous work done by Drougkas et al.,[4]. The steel reinforcing bars, which are placed in pairs in some of the bed joints, are modelled as one single equivalent reinforcement bar with a circular cross-section equal to the sum of the areas of the original bars. Thus, while the diameter of a single steel bar is 6 mm, the diameter of the equivalent steel bar is 8.49 mm. The diagonal ties which are placed at the corners of the window opening in the experiment are excluded in the numerical models in this paper, as these have not been found to have a significant effect on the force capacity and the crack pattern of the wall [4,18]. Furthermore, the steel beams of the supporting frame (represented with beam elements) are kept linear elastic and set in a cantilever configuration; clamped at the base and unrestrained at the top, allowing free rotation of the top beam.

Following the application of the overburden (12 N/mm) and the self-weight, the lateral loading is applied using displacement-control in order to capture the post-peak response. Both cyclic and monotonic pushover analyses have been adopted for the lateral loading. However, to reduce the computational costs for the cyclic pushover analyses, the adopted loading protocol from the experiment has been reduced to only one run per cycle.

The walls have been modelled in 2D and analyzed under plane-stress assumptions using linearly interpolated elements. The reason for this is to simplify the problem since the focus is on the in-plane seismic response of the wall. Therefore, out-of-plane effects are not considered in the models. The applied integration scheme for the line interface elements, plane stress elements and truss elements are 2-point Newton Cotes integration scheme, 2x2 Gauss integration scheme and 1-point Gauss integration scheme, respectively. Considering the analyses up to near collapse, full Newton-Raphson scheme has been applied as the convergence solution method with force and displacement norms (both satisfied) for all models. Different convergence tolerances, varying between 0.01 and 0.02, and load-step sizes were required for each model to be able to find converging results. Additionally, for the continuum damage model, head joint failure is considered via calculation of the tensile strength from the frictional shear stress in the bed joint, as this allows for the effect of high overburden loads to be accounted for in the model. Considering the analyses in the damage limitation phase, a sensitivity study regarding element type, mesh size, step size and convergence solution method was carried out to set the various modelling choices. For a detailed description of these applied numerical settings the reader is referred to Lee [13]. The applied material properties for each model are listed in Table A1. and Table A2. in the Appendix.

4. Numerical results and discussion

4.1. Damage limitation state

In this section, the numerical results of all three modelling approaches are compared with each other as well as with the experimental results. The comparison is done by interpreting the force–displacement curves and the crack patterns at the end of the damage limitation phase (maximum displacement + 1.93 and −1.93 mm in positive and negative loading direction, respectively).

For the *un-strengthened wall*, all numerical models can reproduce the experimental crack pattern in the positive loading direction with very good accuracy (Fig. 3). Considering the negative loading direction, the crack patterns differ slightly between the models and the experiment especially at the bottom right corner of the wall. A possible explanation for this could be the difference in type of unloading, namely secant versus elastic unloading, considered by the different constitutive models. Some differences can also be observed between the models for the crack at the top of the left pier (crack number 2). This is comparable with the experiments [10] where small differences for this crack (sometimes horizontal and sometimes diagonal) were also observed between specimens with the same geometry, material properties, loading and boundary conditions. However, the cracks at the main positions are simulated very accurately, which captures the initiation of

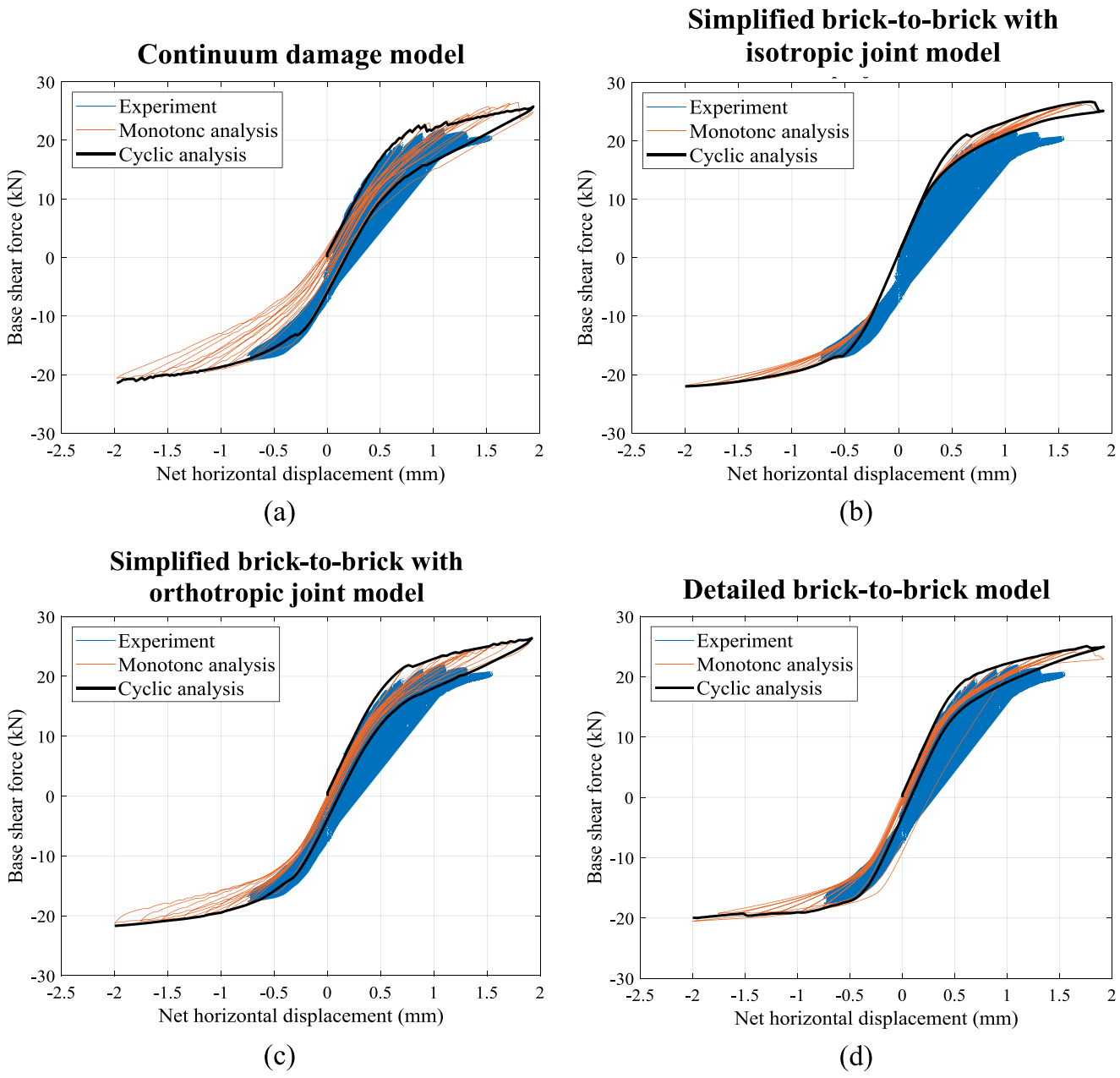

Fig. 4. Comparison of experimental (TUD_COMP-41) and numerical force–displacement curves for un-strengthened wall in damage limitation phase: (a) continuum damage model; (b) simplified brick-to-brick model with isotropic joint model; (c) simplified brick-to-brick model with orthotropic joint model; (d) detailed brick-to-brick model.

Table 1
Maximum base shear force and percentage difference with respect to experimental results for un-strengthened wall.

	Loading	Max. base shear force (kN)		Computational time (min)
		Positive x-direction	Negative x-direction	
Experiment (TUD_COMP-41)	Cyclic (30 run/cycle)	22.05	−18.72	
Continuum damage model	Cyclic (1 run/cycle)	26.47 (+20 %)	−20.94 (+12 %)	4
	Monotonic	25.75 (+17 %)	−21.44 (+15 %)	29
Simplified brick-to-brick model with isotropic joint model	Cyclic(1 run/cycle)	26.24 (+19 %)	−21.91 (+17 %)	58
	Monotonic	26.71 (+21 %)	−22.01 (+18 %)	322
Simplified brick-to-brick model with orthotropic joint model	Cyclic(1 run/cycle)	26.18 (+19 %)	−21.25 (+14 %)	36
	Monotonic	26.38 (+20 %)	−21.70 (+16 %)	276
Detailed brick-to-brick model	Cyclic(1 run/cycle)	24.74 (+12 %)	−20.52 (+10 %)	27
	Monotonic	25.07 (+14 %)	−20.01 (+7%)	359

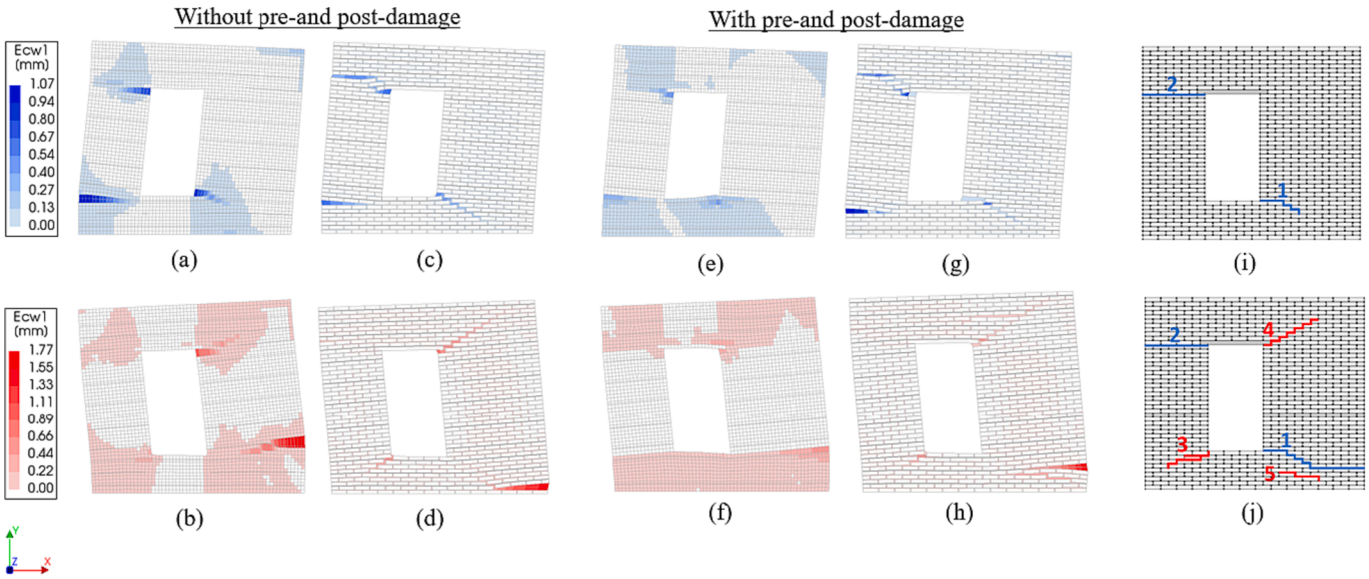

Fig. 5. Crack pattern in positive (blue) and negative (red) loading direction for strengthened wall in Damage Limitations phase: (a)-(b) continuum damage model without pre- and post-damage; (c)-(d) simplified brick-to-brick model with isotropic joint model and without pre- and post-damage; (e)-(f) continuum damage model and with pre- and post-damage; (g)-(h) simplified brick-to-brick model with isotropic joint model and with pre- and post-damage; (i)-(j) experimental results (TUD_COMP-45). Ecw1 is the crack width in the maximum principal direction in plane stress elements. (For interpretation of the references to colour in this figure legend, the reader is referred to the web version of this article.)

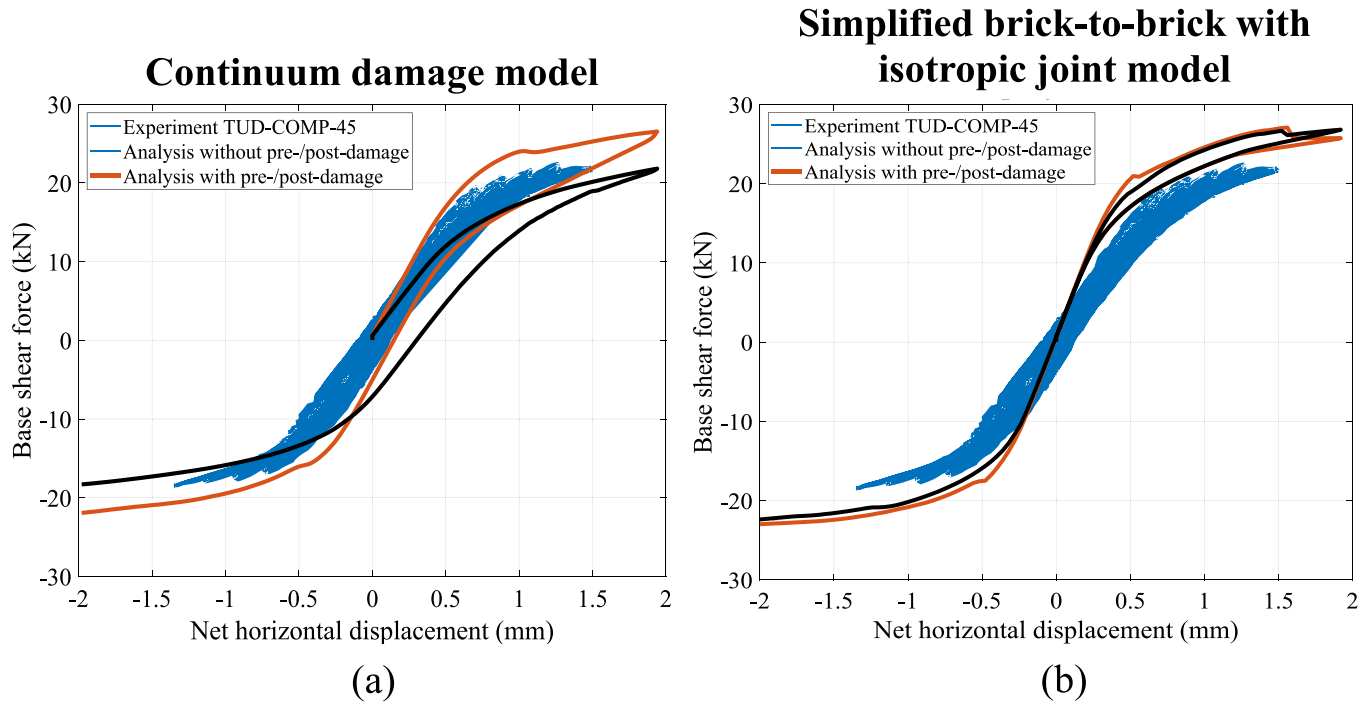

Fig. 6. Comparison of experimental (TUD_COMP-45) and numerical force–displacement curves (monotonic analyses) for strengthened wall with and without pre- and post-damage in Damage Limitation phase: (a) continuum damage model; (b) simplified brick-to-brick model with isotropic joint model.

rocking of both piers. For the simplified brick-to-brick model, the isotropic joint model (Fig. 3*(c)-(d)*) provides better results than the orthotropic joint model (Fig. 3*(e)-(f)*). Specifically, the orthotropic joint model is unable to capture the diagonal staircase cracks as observed in the experiment, and instead mainly displays horizontal cracks. This can possibly be explained by the fact that this material model was mainly developed to simulate masonry as a composite material, for which the orthotropic behavior can be captured by using different properties for the elasticity, strength and toughness.

The numerically derived force–displacement curves (Fig. 4) are in reasonable agreement with the experimental results in terms of the initial stiffness and the maximum force capacity of the wall, in both loading directions. Furthermore, the capacity curves obtained from the monotonic analyses follow the outline of the capacity curves for the cyclic analyses as the envelope curve. A limitation of the isotropic joint model is the underestimation of the energy dissipation, meaning that the hysteretic behavior is not well-captured because the material model does not allow for elastic unloading (only secant). For this reason, the

Table 2
Maximum base shear force and percentage difference with respect to model without pre- and post-damage.

	Pre-and post-damage included	Max. base shear force (*kN*) Positive x-direction	Negative x-direction
Experiment (TUD_COMP-45)	Yes	22.72	−21.10
Continuum damage model	No	26.53	−21.94
	Yes	21.81 (-18 %)	−18.30 (-17 %)
Simplified brick-to-brick model with isotropic joint model	No	27.08	−22.98
	Yes	26.81 (-1%)	−22.38 (-3%)

capacity curve always goes back to the origin after each cycle; this is an acceptable assumption in tension where we have closing of cracks in unloading, but is not an acceptable assumption in shear.

Table 1 shows a comparison in terms of maximum base shear force in both loading direction and computational time. The small over-estimations of the maximum force capacity can be explained by the fact that the numerical models are expected to be stronger due to perfect conditions, whereas imperfections such as weak brick–mortar bonds can occur locally in the wall in the experiment. Regarding the computational costs, the brick-to-brick models have similar performance and require generally 6 to 14 times more time than the continuum damage model.

The numerical results for the *strengthened wall* are presented and discussed next where the performance of each modelling approach is evaluated based on the inclusion of the pre- and post-damage in the model. The results are presented in terms of crack patterns (Fig. 5), force–displacement curves (Fig. 6) and maximum base shear force

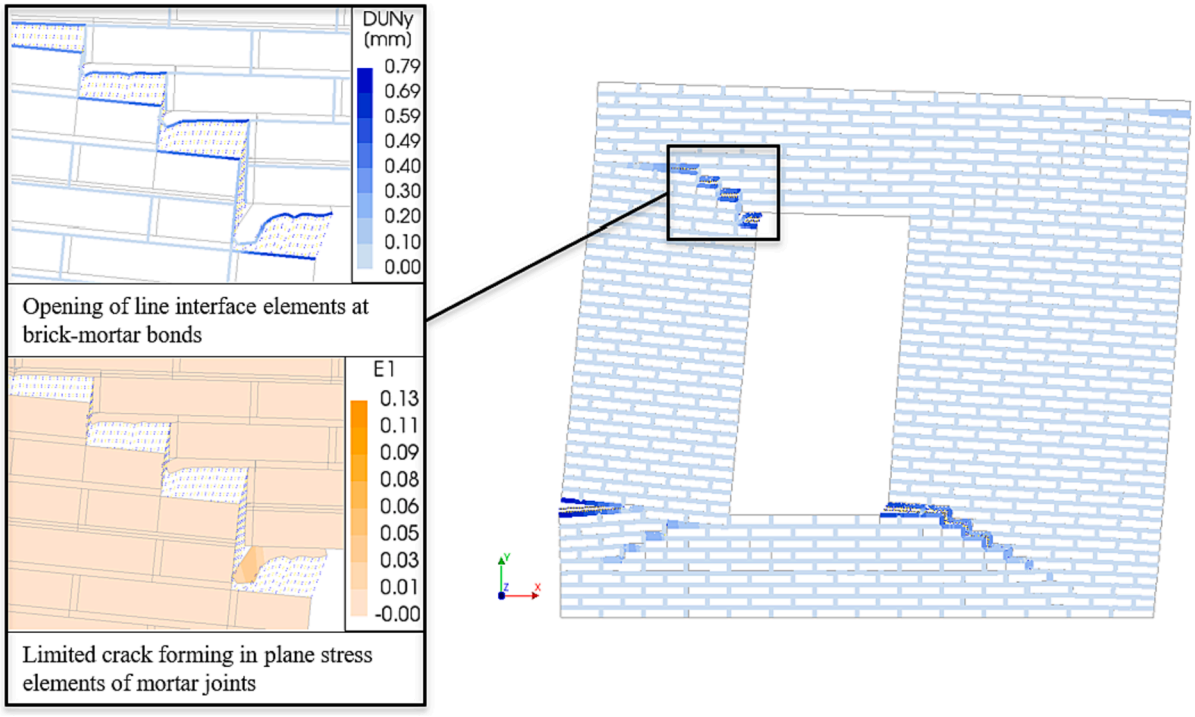

Fig. 7. Crack formation in detailed brick-to-brick model for strengthened wall.

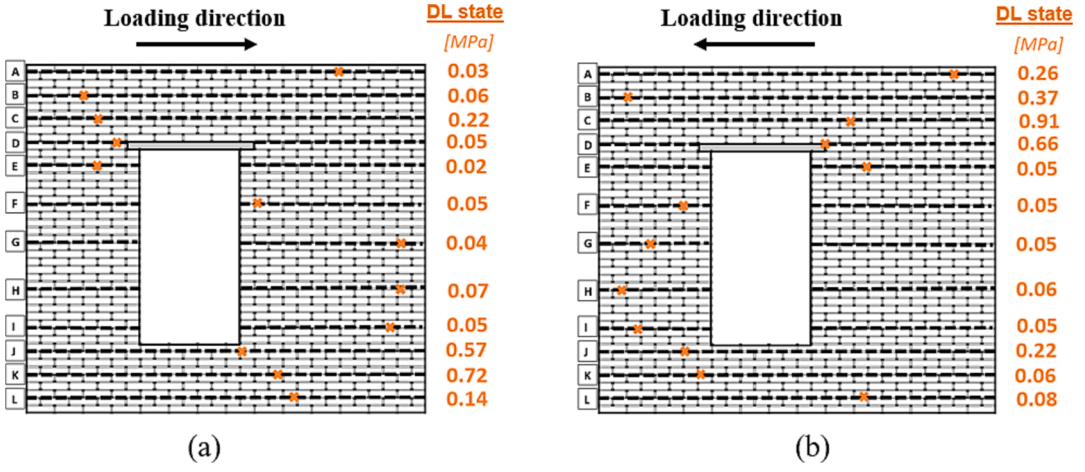

Fig. 8. Maximum axial stress in each row of bed joint reinforcement for detailed brick-to-brick model in Damage Limitation (DL) state: (a) positive loading direction; (b) negative loading direction.

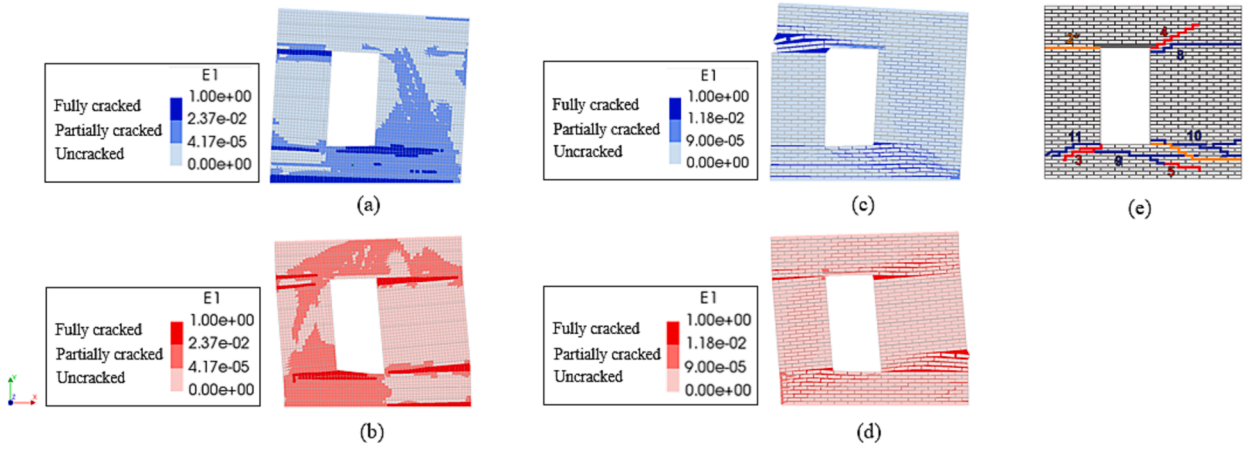

Fig. 9. Crack pattern in positive (blue) and negative (red) loading direction for strengthened wall without pre- and post-damage in Near Collapse phase for: (a)-(b) continuum damage model; (c)-(d) simplified brick-to-brick model with isotropic joint model; (e) experimental results (TUD_COMP-45). (For interpretation of the references to colour in this figure legend, the reader is referred to the web version of this article.)

(Table 2). The results for the simplified brick-to-brick with the orthotropic joint model are not presented here, because as mentioned before with the numerical results of the un-strengthened wall, the model mainly displays horizontal cracks which differs from the experiment. A monotonic pushover loading protocol has been adopted for the analyses of the strengthened wall since, as demonstrated above, the capacity curves obtained from the monotonic analyses follow the outline of the capacity curves for the cyclic analyses as the envelope curve. Moreover, adopting a monotonic analysis for the models significantly reduces the computational demands.

Considering the pre- and post-damage, the *simplified brick-to-brick model* performs better than the *continuum damage model.* For the continuum damage model, the pre- and post-damage is "smeared" over a whole damaged area (Fig. 5*(e)-(f)*) that is larger than the actual localized damaged joints. This means that the wall is expected to be weaker on a larger area thus increasing the discrepancy between experimental and numerical results. On the other hand, this shortcoming is not present when considering the brick-to-brick model as shown by the results of simplified brick-to-brick model with isotropic joint model (Fig. 5*(g)-(h)*). In case the pre- and post-damage is not included, the continuum damage model provides similar results with the simplified brick-to-brick model for the Damage Limitation phase in terms of the crack patterns (Fig. 5*(a)-(d)*) and the maximum base shear forces in both loading directions (Fig. 6 and Table 2).

On the other hand, the *detailed brick-to-brick model* was found unsuitable for simulating masonry walls retrofitted with bed joint reinforced repointing. Cracks mainly occurred in the form of opening of the line interface elements at the brick–mortar bonds, while smeared cracking in the plane stress elements of the mortar joints was very limited (Fig. 7). Since the reinforcement bars are connected to the plane stress elements representing the mortar joints, they experienced limited elongation and no slip. Consequently, the reinforcements were not getting activated and showed lower values of axial stress (Fig. 8) with respect to the simplified brick-to-brick models and the continuum damage model (Fig. 11). In addition to the Discrete Cracking model, the Combined Cracking-Shearing-Crushing model [16] is another material model which was used for the brick–mortar line interface elements in the numerical investigations by Lee [13]. It was concluded that this material model is not accurate for cyclic analyses because of the fact that elastic unloading takes place in tension, resulting in overly stiff cracks which do not close when loading the wall in the opposite direction. The cracks got larger after each cycle which was also seen in the force–displacement curves in the form of an overestimation of the energy dissipation.

4.2. Near collapse state

The response of the *strengthened wall* up to Near Collapse is simulated using only the continuum damage model and the simplified brick-to-brick model with isotropic joint model, since these two models had the most promising results from the tests up to the Damage Limitation state.

The results for the Near Collapse state are compared with each other for both models in terms of the crack patterns (Fig. 9) and force–displacement curves (Fig. 10). The simplified brick-to-brick model with isotropic joint model is able to capture the diagonal stair-case cracks (Fig. 9*(c)-(d)*), whereas the cracks in the continuum damage model are mainly horizontal (Fig. 9*(a)-(b)*).

The maximum force capacity of the wall is overestimated in both loading directions for both models as can be observed in the numerically derived force–displacement curves (Fig. 10). The strengthened wall *TUD_COMP-45* showed a maximum base shear force equal to + 25.14 kN and –23.46 kN in the positive and negative loading directions, respectively [28], while the numerically-derived results and corresponding percentage differences with respect to the experiment are: +28.73 kN (+14 %) and −25.82 kN (+10 %) in the positive and negative loading direction, respectively for the continuum damage model and + 27.26 kN (+8%) and −26.27 kN (+12 %) in the positive and negative loading direction, respectively for the simplified brick-to-brick-model with isotropic joint model. After the peak, the numerical results are obtained with a converging error closer to the specified convergence tolerance (0.01 for continuum damage model and 0.02 for simplified brick-to-brick model), as indicated by orange markers in Fig. 10. However, in some cases the error is relative larger (>0.05), as indicated by red markers in Fig. 10; this is especially around at a displacement of + 50 mm when a horizontal crack at the base of the wall is formed, as shown for the continuum damage model in Fig. 10*(a)* and for the simplified brick-to-brick model in Fig. 9*(c)*.

The maximum axial stresses occurring in each row of bed joint reinforcement are indicated in Fig. 11 for both models in the Damage Limitation state (orange) as well as in the Near Collapse state (black). Important to note is that the maximum axial stresses in each row of rebars are not reached at the same top displacement of the wall. It can be observed that the axial stresses in the rebars are overall higher in the simplified brick-to-brick model with isotropic joint model than the continuum damage model. A possible explanation for this is that the brick-to-brick model does allow for the direct assignment of material properties for the high strength repair mortar in the strengthened joints, while the continuum damage model does not. Consequently, the strengthened joints are stiffer in the simplified brick-to-brick model and

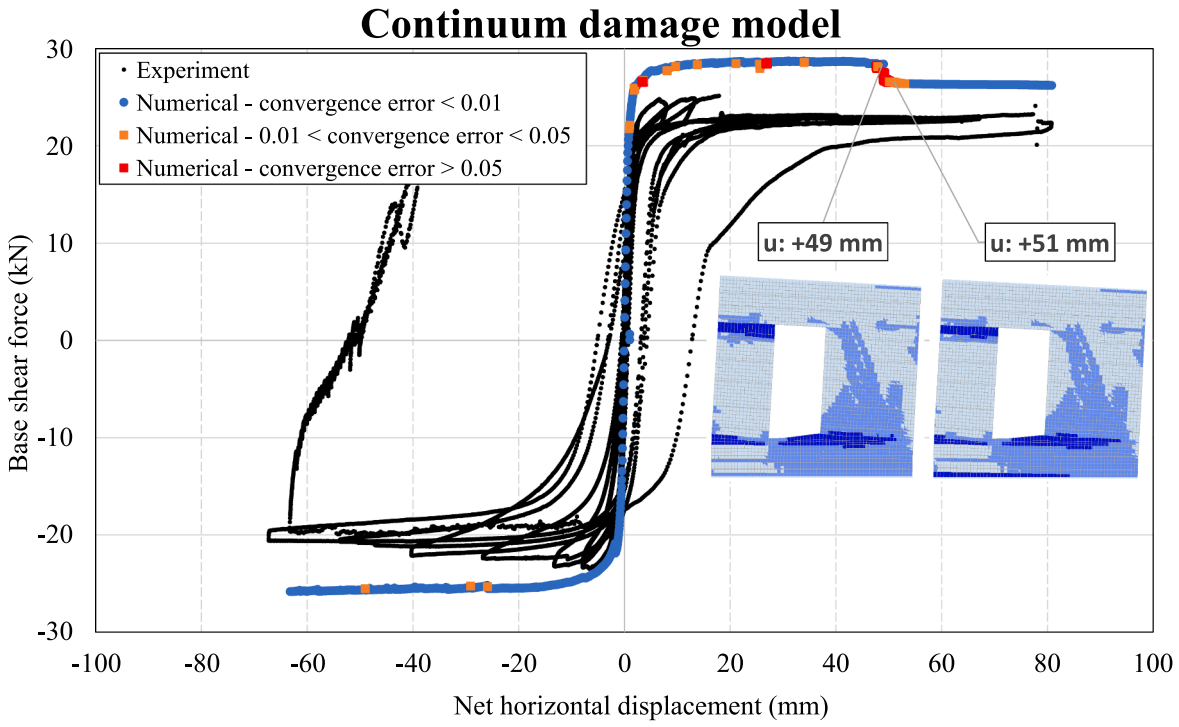

(a)

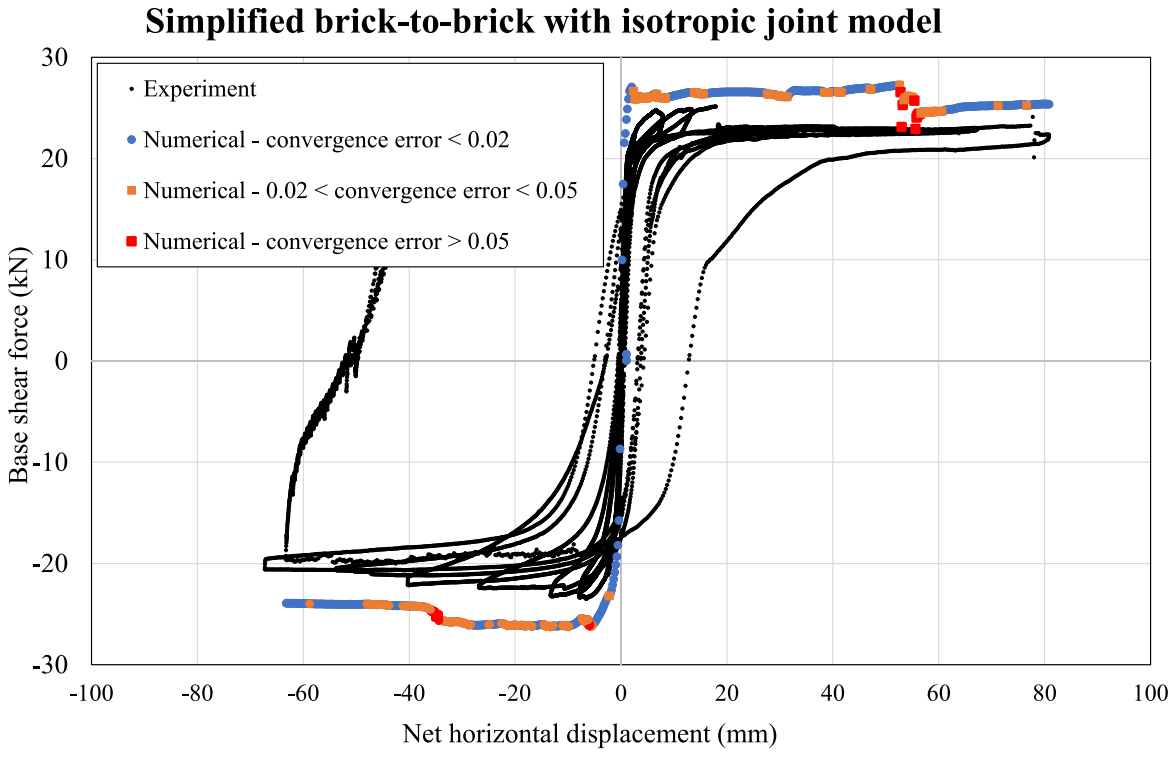

(b)

Fig. 10. Comparison of experimental (TUD_COMP-45) and numerical force–displacement curves (monotonic analyses) for strengthened wall without pre- and post-damage in Near Collapse: (a) continuum damage model; (b) simplified brick-to-brick model with isotropic joint model.

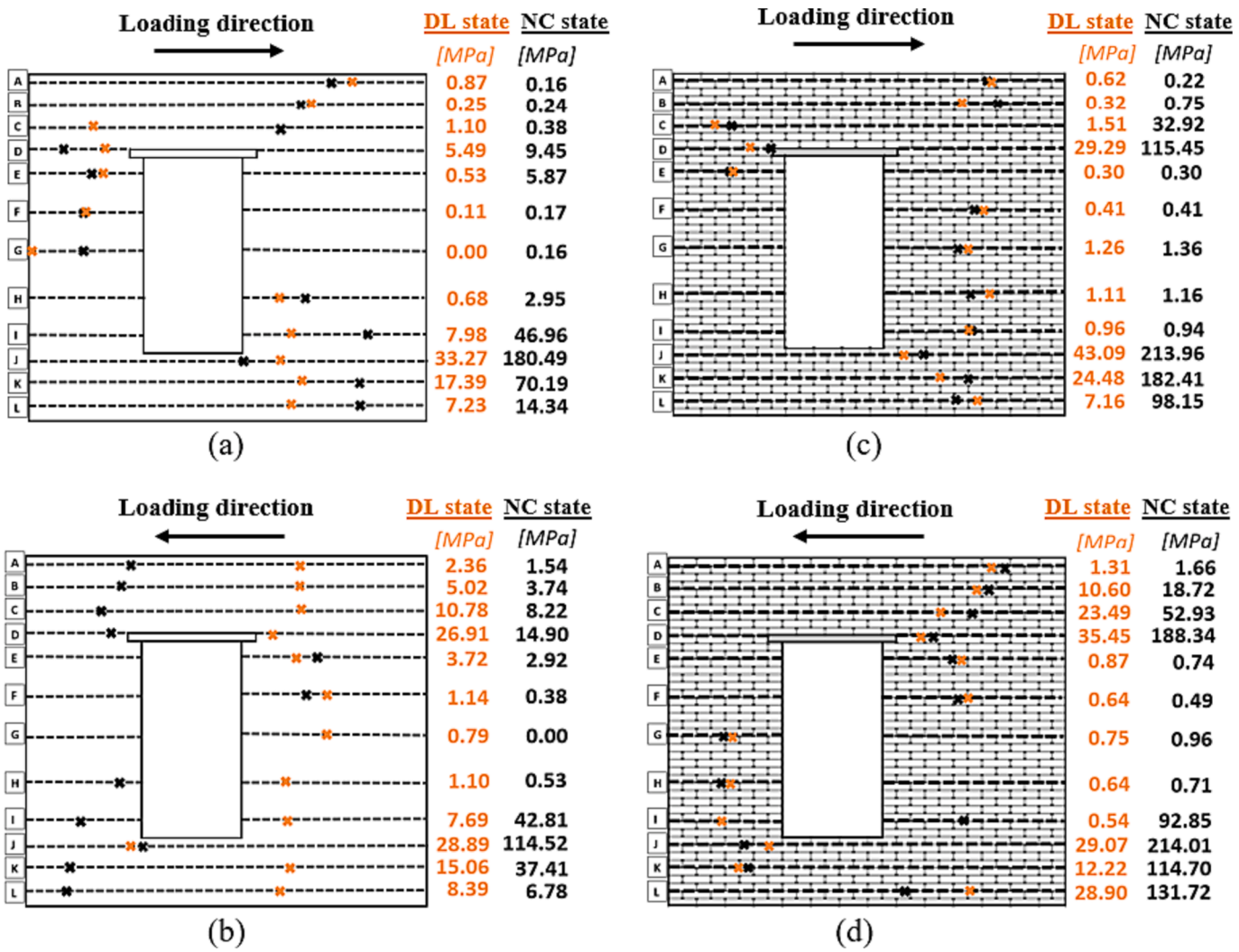

Fig. 11. Maximum axial stress in each row of bed joint reinforcement for Damage Limitation state (orange) and Near Collapse state (black): (a)-(b) continuum damage model; (c)-(d) simplified brick-to-brick model with isotropic joint model. (For interpretation of the references to colour in this figure legend, the reader is referred to the web version of this article.)

thus the axial stresses are higher in the rebars.

5. Conclusions

In this paper three different modelling approaches for simulating un-strengthened and strengthened full-scale masonry walls retrofitted with bed joint reinforced repointing were investigated. Each approach simulated the wall at different levels of detail, ranging from the *continuum damage model,* in which the bricks and mortar joints are modelled as one homogenous continuum, to the *simplified* and *detailed brick-to-brick models,* in which the bricks and mortar joints are modelled separately (with line interface elements at the brick–mortar bonds for the latter model). The objective of this study was to compare the accuracy of the modelling approaches and to determine the most suited especially for the simulation of the strengthened wall, also considering the comparison for the un-strengthened one.

Considering the simulations of the un-strengthened wall, all modelling approaches are able to reproduce the experimental crack pattern with very good accuracy and provide an estimation of the base shear force within a maximum of 20 % error. The cracks at the main positions are simulated very accurately, which captures the rocking failure behavior of both piers. However, the brick-to-brick models offer greater resolution in modelling the crack pattern compared to the continuum damage model. This comes at the cost of modelling and computational time, with the latter being 6 to 14 times larger than the one required by the continuum damage model.

Among the simplified brick-to-brick models, the *isotropic joint model* is able to reproduce the experimental crack pattern more accurately compared with the *orthotropic joint model*. However, only the latter model is able to capture the hysteretic behavior in the force–displacement curve since the material model allows for elastic unloading in shear.

Considering the simulations of the strengthened wall, the *detailed brick-to-brick model* is not able to capture the behavior of the reinforcements since cracks mainly occur in the form of opening of the brick–mortar interface elements, while cracking in the plane stress elements representing the mortar joints is very limited. Consequently, the reinforcements are not getting activated and thus inaccurate/low values are obtained for the axial stress.

If pre- and post-damage needs to be included in the model, the *simplified brick-to brick model* is more accurate compared with the *continuum damage model* since the geometry of the bed and head joints are modelled separately which allows for the direct assignment of the modified material properties to each structural component. On the other hand, if pre- and post-damage is not simulated, both models provide similar results for the analyses in the Damage Limitation phase but not

Table A1
Material properties for different mortar joints in simplified and detailed brick-to-brick model adopted from Drougkas et al., [4] and Korswagen et al., (2019).

Property	Symbol	Unit	Bed joints	Head joints	Strengthened bed joints	Repaired bed joints	Pre-/post-damaged bed joints	Pre-/post-damaged head joints
Young's modulus	E	N/mm^2	1000[b]	500[a]	6630[d]	6315[d]	500[e]	250[e]
Poisson's ratio	ν	–	0.14[a]	0.14[a]	0.14[a]	0.14[a]	0.14[a]	0.14[a]
Mass density	ρ	kg/m^3	1708[a]	1708[a]	1708[a]	1708[a]	1708[a]	1708[a]
Tensile strength	f_t	N/mm^2	0.09[a]	0.05[b]	0.09[d]	0.032[d]	0	0
Tensile fracture energy	G_f^I	N/mm	0.00753[c]	0.00499[c]	0.00753[d]	0.003[d]	0	0
Compressive strength	f_c	N/mm^2	12.93[a]	3.81[a]	20.72[d]	20.72[d]	12.93[a]	3.81[a]
Compressive fracture energy	G_c	N/mm	28.63[b]	6.4[b]	82.75[d]	82.75[d]	28.63[b]	6.4[b]
Shear modulus	G_{xy}	N/mm^2	439[b]	219[b]	2908[b]	2770[b]	219[b]	110[b]
Friction angle	φ	rad	0.6686[a]	0.6686[a]	0.6686[a]	0.6686[a]	0.6686[a]	0.6686[a]
Cohesion	c	N/mm^2	0.13[a]	0.13[a]	0.13[a]	0.13[a]	0.13[a]	0.13[a]
Fracture energy in shear	$G_{v,i}$	N/mm	0.3[b]	0.3[b]	0.3[b]	0.3[b]	0	0

[a] From companion tests (material characterization).
[b] From calibration
[c] From formulation ([27]).
[d] From formulation according to the rule of mixture [4].
[e] From assumption [4].

for the Near Collapse phase. The cracks in the continuum damage model are mainly horizontal, while the simplified brick-to-brick model is able to reproduce the diagonal (staircase) cracks with a higher degree of fidelity. Moreover, the maximum axial stresses in the rebars are overall higher in the simplified brick-to-brick model, which can be possibly explained by the fact that the model allows for the direct assignment of material properties for the high strength repair mortar in the strengthened joints.

One limitation of the applied models in this study is that the out-of-plane (OOP) deformation cannot be captured since the models are two-dimensional. According to [4,28], OOP deformation in the strengthened wall was observed towards the end of the test, not only at the base of the wall but also in both piers due to the asymmetric placement of the bed joint reinforcements within the thickness of the wall. The OOP effect can be simulated with the use of layered shell elements, which was applied by Drougkas et al., [4]. Important to emphasize however is that computational costs will be significantly increased. Furthermore, the bricks are kept linear elastic in the brick-to-brick models in this study, which means that the possibility of crushing and cracking in the bricks are ignored. This assumption was made considering that mostly tensile and shear failure in joints was experimentally reported. Moreover, it reduces the computational costs significantly. This approach remains valid up to the point where the bricks experience local failure (crushing and cracking), which was at the last cycle of the experiment for the strengthened wall at the bottom right corner.

Finally, different application fields exist for the different modelling approaches examined here. The two brick-to-brick models are necessary to give a better understanding about the local failure behavior in masonry, while the continuum damage model is better suited when a compromise between accuracy and efficiency is needed - for example, when modelling entire structures instead of individual structural components.

CRediT authorship contribution statement

Ka Ho Lee: Methodology, Visualization, Formal analysis, Writing - original draft. **Anjali Mehrotra:** Conceptualization, Supervision, Writing – review & editing. **Rita Esposito:** Conceptualization, Supervision, Writing – review & editing.

Declaration of Competing Interest

The authors declare that they have no known competing financial interests or personal relationships that could have appeared to influence the work reported in this paper.

Table A2
Material properties for continuum damage model adopted from Korswagen et al., (2019).

Property	Symbol	Value	Unit
Young's modulus	E_x	2157[b]	N/mm^2
	E_y	3087[a]	N/mm^2
Shear modulus	G_{xy}	1354[b]	N/mm^2
Mass density	ρ	1708[a]	kg/m^3
Tensile strength	f_t	0.09[a]	N/mm^2
Fracture energy in tension	G_f^I	0.007527[c]	N/mm
Compressive strength	f_c	11.35[a]	N/mm^2
Fracture energy in compression	G_c	26.05[a]	N/mm
Friction angle	φ	0.669[a]	rad
Cohesion	c	0.14[a]	N/mm^2
Angle between stepped diagonal crack and bed-joint	α	0.5[a]	rad

[a] From companion tests (material characterization).
[b] From calibration
[c] From formulation ([27]).

Data availability

Data will be made available on request.

Acknowledgement

This work was partially developed as MSc graduation project of the first author. For their participation in the graduation committee and feedback during progress meetings, the authors wish to thank Prof. Dr Jan Rots and Dr Geert J.P. Ravenshorst.

Appendix

References

[1] Bertolesi E, Milani G, Fagone M, Rotunno T, Grande E. Micro-mechanical FE numerical model for masonry curved pillars reinforced with FRP strips subjected to single lap shear tests. Compos Struct 2018;201:916–31.
[2] D'Altri AM, de Miranda S, Castellazzi G, Sarhosis V. A 3D detailed micro-model for the in-plane and out-of-plane numerical analysis of masonry panels. Comput Struct 2018;206:18–30.

[3] Drougkas A, Licciardello L, Rots JG, Esposito R. In: Experimental and numerical study of historic masonry with bed joint reinforced repointing. European Association for Structural Dynamics (EASD); 2020. p. 4212–25.
[4] Drougkas A, Licciardello L, Rots JG, Esposito R. In-plane seismic behaviour of retrofitted masonry walls subjected to subsidence-induced damage. Eng Struct 2020;223:111192.
[5] federation internationale du beton (*fib*). (2010). Model Code for Concrete Structures 2010.
[6] D. Ferreira 2020 User's manual—Release 10.4. Diana User's Manual. https://manuals.dianafea.com/d104/Diana.html.
[7] Ghiassi B, Oliveira DV, Lourenço PB, Marcari G. Numerical study of the role of mortar joints in the bond behavior of FRP-strengthened masonry. Compos B Eng 2013;46:21–30.
[8] Green RA, Bommer JJ, Stafford PJ, Maurer BW, Kruiver PP, Edwards B, et al. Liquefaction hazard in the Groningen region of the Netherlands due to induced seismicity. J Geotech Geoenviron Eng 2020;146(8).
[9] Hafnerq I, Kišiček T, Gams M. Improving the seismic response of masonry piers with single-sided FRCM coating using clamping details–numerical modelling. In International Conference on Structural Analysis of Historical Constructions (SAHC2023) 2023:1189–201.
[10] Korswagen PA, Longo M, Meulman E, Rots JG. Crack initiation and propagation in unreinforced masonry specimens subjected to repeated in-plane loading during light damage. Bull Earthq Eng 2019;17(8):4651–87.
[11] P.A. Korswagen M. Longo E. Meulman Damage sensitivity of Groningen masonry structures - Experimental and computational studies - Stream 2 - Part 1. 2019 Report number C31B69WP0-14, Report, version 2.0.
[12] Korswagen PA, Longo M, Rots JG. High-resolution monitoring of the initial development of cracks in experimental masonry shear walls and their reproduction in finite element models. Eng Struct 2020;211:110365.
[13] Lee K. A comparison study of numerical modeling approaches for simulating the in-plane seismic reponse of masonry walls. Delft University of Technology: MSc thesis 2022.
[14] Licciardello, L., Rots, J.G., Esposito, R. Performance of unreinforced masonry strengthened with bed joint reinforced repointing 2020; In proceedings of 25th International Conference on Structural Analysis of Historical Constructions, Barcelona, Spain.
[15] Lotfi HR, Shing PB. Interface model applied to fracture of masonry structures. J Struct Eng 1994;120(1):63–80.
[16] Lourenço PB, De Borst R, Rots JG. A plane stress softening plasticity model for orthotropic materials. Int J Numer Meth Eng 1997;40(21):4033–57.
[17] Lourenço PB, Rots JG, Blaauwendraad J. Two approaches for the analysis of masonry structures: Micro and macro-modeling. HERON 1995;40(4):1995.
[18] S. Mahmoudimotlagh Numerical Modeling of the In-Plane Seismic Behavior of Unreinforced Masonry Wall Retrofitted with Bed Joint Reinforcements. Delft University of Technology: MSc thesis. 2020.
[19] Messali F, Esposito R, Ravenshorst GJP, Rots JG. Experimental investigation of the in-plane cyclic behaviour of calcium silicate brick masonry walls. Bull Earthq Eng 2020;18(8):3963–94.
[20] Messali, F., Ravenshorst, G.J.P., Esposito, R., Rots, J.G. Large-scale testing program for the seismic characterization of Dutch masonry walls 2017, In Proceedings of 16th world conference on earthquake (WCEE), Santiago, Chile.
[21] Messali F, Rots JG. In-plane drift capacity at near collapse of rocking unreinforced calcium silicate and clay masonry piers. Eng Struct 2018;164:183–94.
[22] Murgo FS, Ferretti F, Mazzotti C. A discrete-cracking numerical model for the in-plane behavior of FRCM strengthened masonry panels. Bull Earthq Eng 2021;19(11):4471–502.
[23] Rots JG. Numerical simulation of cracking in structural masonry. Heron 1991;36(2):49–63.
[24] Rots JG. Structural masonry: An experimental/numerical basis for practical design rules. CRC Press; 1997.
[25] Rots JG, De Borst R. Analysis of mixed-mode fracture in concrete. J Eng Mech 1987;113(11):1739–58.
[26] Rots JG, Messali F, Esposito R, Jafari S, Mariani V. Computational modelling of masonry with a view to Groningen induced seismicity. In: Van Balen K, Verstrynge E, editors. Structural Analysis of Historical Constructions: Anamnesis, diagnosis, therapy, controls -. CRC Press / Balkema - Taylor & Francis Group; 2016. p. 227–38.
[27] Schreppers GMA, Garofano A, Messali F, Rots JG. DIANA validation report for masonry modelling. DIANA FEA Report 2016-DIANA-R1601 TU Delft Structural Mechanics Report CM-2016-17. 2016.
[28] Licciardello L, Rots JG, Esposito R. Experimental tests on masonry strengthened with bed joint reinforced repointing. Heron 2021;66(1):61–90.